• Basic Research •

Vaccinia-related kinase 1/snail family transcriptional repressor 1 regulates epithelial-mesenchymal transition and inflammation in proliferative vitreoretinopathy

Ying Ying[1], *Xin Liao*[2]

[1]Ophthalmology Department, Shanghai Eighth People's Hospital, Shanghai 200235, China
[2]Ophthalmology Department, Shanghai Tenth People's Hospital Affiliated to Tongji University, Shanghai 200072, China
Correspondence to: Xin Liao. Ophthalmology Department, Shanghai Tenth People's Hospital Affiliated to Tongji University, 15th Floor, Building 1, No.301, Yanchang Middle Road, Jing'an District, Shanghai 200072, China. liaoxin759@hotmail.com
Received: 2025-09-11 Accepted: 2025-11-03

Abstract
● **AIM:** To investigate whether vaccinia-related kinase 1 (VRK1) mediates transforming growth factor-beta2 (TGF-β2)-caused epithelial-mesenchymal transition (EMT) and inflammatory responses in retinal pigment epithelial (RPE) cells through regulating snail family transcriptional repressor 1 (SNAI1), and to validate its role in a proliferative vitreoretinopathy (PVR) mouse model.
● **METHODS:** Human RPE cell line ARPE-19 cells were treated with TGF-β2 to construct an EMT model. Western blot detected VRK1 level. The effects of VRK1 on SNAI1 expression and biological behavior of ARPE-19 cells were detected by immunofluorescence, ELISA, Transwell, and scratch assay, and the interaction between VRK1 and SNAI1 was confirmed through immunoprecipitation. A PVR mouse model was constructed, and the effects of VRK1 or/and SNAI1 on retinal damage were assessed by pathologic staining. Inflammatory factors and EMT-related proteins were assessed with ELISA and Western blot.
● **RESULTS:** VRK1 was upregulated in ARPE-19 cells after TGF-β2 treatment. Overexpression of VRK1 increased cell viability, promoted cell migration and EMT, and the levels of inflammatory factors. Silencing of VRK1 reversed the above indexes. There was a direct interaction between VRK1 and SNAI1, and overexpresssion SNAI1 weakened the impacts of silencing of VRK1. In PVR mice, silencing of VRK1 ameliorated retinal structural damage, decreased proinflammatory factor levels, and suppressed SNAI1 and mesenchymal marker expression. SNAI1 overexpression antagonized the protective effects of silencing VRK1 and exacerbated EMT and inflammatory responses.
● **CONCLUSION:** VRK1 plays a key role in retinal structural and inflammatory damage in PVR mice by regulating SNAI1 and mediating TGF-β2-caused EMT and inflammatory responses in RPE cells.
● **KEYWORDS:** proliferative vitreoretinopathy; vaccinia-related kinase 1; epithelial-mesenchymal transition; inflammation; snail family transcriptional repressor 1; retinal pigment epithelial cells; mice
DOI:10.18240/ijo.2026.03.03

Citation: Ying Y, Liao X. Vaccinia-related kinase 1/snail family transcriptional repressor 1 regulates epithelial-mesenchymal transition and inflammation in proliferative vitreoretinopathy. *Int J Ophthalmol* 2026;19(3):443-454

INTRODUCTION
Proliferative vitreoretinopathy (PVR) is a blinding disease of the fundus of the eye that commonly occurs after foramen ovale retinal detachment, ocular trauma, and internal eye surgery[1-2]. About 5% to 11% of patients with foramen ovale retinal detachment will develop PVR[3]. PVR characterized pathologically by the abnormal proliferation of retinal pigment epithelium (RPE) cells, leading to the formation of fibrous scar tissue[4-5]. Currently, PVR treatment is still based on vitrectomy and scleral buckling, but the surgery can only lift the mechanical traction and cannot fundamentally block the fibrosis process[6-7]. Consequently, in-depth analysis of PVR pathogenesis to block the process of PVR are key issues to improve postoperative visual function.
The pathogenesis of PVR is intricate, with the involvement of growth factors, cytokines, extracellular matrix and multiple cellular interactions[8-9]. Epithelial-mesenchymal transition (EMT) of RPE cells is a central event driving fibrous scar formation[10-12]. Stimulated by pathological factors such as transforming growth factor-β2 (TGF-β2), RPE cells gradually

lose epithelial polarity, and secrete extracellular matrix proteins to form a fibroproliferative membrane, ultimately exacerbating retinal detachment[13-14]. The EMT process is regulated by a network of transcription factors, among which snail family transcriptional repressor 1 (SNAI1) acts as a major transcription factor, and up-regulation SNAI1 promotes EMT in RPE cells[15]. Additionally, the release of pro-inflammatory factors in retinal tissue further exacerbates the EMT process and PVR progression[13,16]. Thus, it is crucial to examine the primary molecular pathways and regulatory factors during the EMT process in RPE cells.

Vaccinia-related kinase 1 (VRK1) is essential for DNA damage repair and immune response[17-18]. Inhibition of VRK1 expression hinders the abnormal migration and proliferation of vascular smooth muscle cells, which in turn inhibits neointimal hyperplasia[19]. Notably, in a hepatocellular carcinoma model, VRK1 promotes SNAI1 expression by phosphorylating the chromatin deconjugating enzyme CHD1L to drive the EMT process[20]. However, whether VRK1 affects the progression of PVR by regulating SNAI1 has not been reported. Therefore, we constructed a EMT model of RPE cells and a PVR mouse model to investigate the impact of VRK1 on PVR progression. This study aims to refine the theory of PVR pathogenesis and to provide an experimental foundation for PVR treatment.

MATERIALS AND METHODS

Ethical Approval This research was granted approval by the Experimental Animal Ethics Committee of Shanghai Eighth People's Hospital (Approval number: D202510-2).

Cell Culture and Processing Human RPE cell line ARPE-19 (SNL-227) was from Sunncell Biotechnology (Wuhan, Hubei Pronvince, China), grown in DMEM/F12 complete medium (SNM-004E, Sunncell Biotechnology) at 37°C with 5% CO_2. Cells were digested with 0.25% trypsin solution (T4049, Sigma-Aldrich, St. Louis, MO, USA), and passaging was carried out at a ratio of 1:3.

ARPE-19 cells were exposed to TGF-β2 (20 ng/mL, HY-P7119, MedChemExpress, Monmouth Junction, NJ, USA) for 24h to establish an EMT model[21]. ARPE-19 cell morphology was observed with a CX33 light microscope (Olympus, Tokyo, Japan)[22]. VRK1 overexpression plasmid (OE-VRK1), VRK1 small interfering RNA (si-VRK1), SNAI1 overexpression plasmid (OE-SNAI1), and control plasmids (OE-NC, si-VRK1) were synthesized by RiboBio Co., Ltd. (Guangzhou, Guangdong Pronvince, China). Using Lipofectamine 3000 (L3000150, Invitrogen, Carlsbad, CA, USA) to transfect the above plasmids into ARPE-19 cells, respectively. After 48h of transfection, the effectiveness of the transfection was assessed by measuring VRK1 or SNAI1 levels. After confirming the successful transfection of OE-VRK1/si-VRK1/OE-SNAI1 in ARPE-19 cells, the cells were exposed to TGF-β2 for 24h to induce EMT.

Cell Counting Kit-8 Assay ARPE-19 cells were inoculated into 96-well plates (5×10^3 cells/well). After the cells were adhered to the wall overnight, 100 μL of medium containing cell counting kit-8 (CCK-8) reagent (10%, HY-K0301, MedChemExpress) was introduced, and incubated for 2h at 37°C. OD_{450} values were examined using a 1410101 microplate reader (Thermo Fisher Scientific, Waltham, MA, USA).

EdU Staining ARPE-19 cells were inoculated in 6-well plates (with built-in sterile coverslips) and gently washed twice with PBS. 5-Ethynyl-2'-deoxyuridine (EdU) working solution (10 μmol/L, ab219801, Abcam, Cambridge, MA, USA) was introduced to cover the cells in the dark for 2h[23]. Cells were exposed to 4% paraformaldehyde (HY-Y0333, MedChemExpress) for 15min, treated with 0.3% Triton X-100 (T824275, Macklin, Shanghai, China) for 10min, then treated with Click reaction solution for 30min. The cell slides were blocked with AntiFade mounting medium (containing DAPI, HY-K1047, MedChemExpress), visualized using a DM3000 fluorescence microscope (Leica, Heidelberg, Germany).

Scratch-Wound Assay ARPE-19 cells were inoculated in 6-well plates (1.0×10^6 cells/well). After cultivation until the cell confluence reached 80%-90%, the tip of a 20 μL pipette was used to draw a straight line on the cell monolayer perpendicular to the edge of the 6-well plate. After being washed with phosphate buffered saline (PBS), serum-free medium was added, and the scratch healing was observed microscopically after 24h. Finally, the scratch healing area was analyzed using Image J 1.54h software (Wavne Resband, National Institute of Mental Health, USA).

Transwell Assay Added the DMEM/F12 complete medium (600 μL) into the 24-well plate. Transwell chambers (8 μm, Corning, Tewksbury, MA, USA) were then placed in 24-well plates, 100 μL ARPE-19 cell suspension (3×10^5/mL) was added into the upper chamber and incubated for 24h. The medium was aspirated, and the unmigrated cells on the Transwell were removed using a sterilized cotton swab. Subsequently, the chambers were immersed in 4% paraformaldehyde (P885233, Macklin) for 10min. Migrating cells were dyed with 0.1% crystal violet (C916088, Macklin) for 15min and then rinsed with PBS. Five randomly selected fields of view were imaged using a microscope and the migrating cells was counted.

Immunofluorescence ARPE-19 cells were inoculated into 12-well plates and cultured for 24h, immersed in 4% paraformaldehyde for 25min, and then incubated with 0.3% Triton X-100 solution for 15min at 25°C. After washing with PBS, they were blocked with 5% bovine serum protein (BSA, A801320, Macklin) for 30min. Added FITC-labeled Phalloidin solution (200 μL, P5282, Sigma-Aldrich) and incubated overnight at 4°C to stain the cytoskeleton[24].

Additionally, cells were incubated overnight with primary antibodies SNAI1 (MA5-14801, 1:250, Invitrogen), alpha smooth muscle actin (α-SMA, ab124964, 1:250, Abcam), or Collagen I (PA1-26204, 1:100, Invitrogen) at 4°C, then incubated with goat anti-rabbit IgG (F-2765, 1:100, Invitrogen) for 1.5h in the dark. After washing with PBS, cells were blocked with AntiFade Mounting Medium (containing DAPI) and observed under a fluorescence microscope.

Co-immunoprecipitation Assay The interaction of VRK1 with SNAI1 was verified using the Pierce Classic Magnetic immunoprecipitation/co-immunoprecipitation (IP/Co-IP) Kit (88804, Thermo Fisher Scientific)[25-26]. HA-SNAI1 and Flag-VRK1 were transfected into ARPE-19 cells for 24h, cells were lysed using IP lysis/washing buffer. Cell lysates were treated with the HA-SNAI1 (1:50, MA5-14801, Invitrogen) and Flag-VRK1 antibody (1:100, PA5-81115, Invitrogen) at 4°C for 12h. The A/G beads were mixed, washed with lysis/washing buffer, and the beads were collected with a magnetic rack. The mixture after having been incubated overnight with the antibody was mixed with the A/G magnetic beads and incubated for 1h at 25°C. The beads were collected and rinsed with lysis/wash buffer. Finally, it was eluted with 100 μL of elution buffer, the eluate was collected, 10 μL of neutralization solution was added, and Western blot was performed.

PVR Mouse Model C57BL/6J mice (8 weeks old, male, 20-25 g) were from Vitalriver (Beijing, China), housed at 22°C±2°C, 12h light and dark alternation, 45%-55% humidity. After 1wk of acclimatization, the mice were split into Control, PVR, PVR+si-NC, PVR+si-VRK1, PVR+si-VRK1+OE-NC, and PVR+si-VRK1+OE-SNAI1 groups in a random manner (n=8). Dispase (0.15 U, 2 μL, I2512, Sigma-Aldrich) was injected intravitreally under a microscope into the left eye of mice 1.5 mm from the corneal limbus to induce PVR[27-28]. Control group mice were injected with saline only. Adeno-associated virus serotype 2 (AAV2; NovoPro Biotechnology, Shanghai, China) was used to overexpress SNAI1 or silence VRK1 in mice. After dispase injection, AAV-si-NC, AAV-si-VRK1, AAV-si-VRK1 and AAV-OE-NC, AAV-si-VRK1 and AAV-OE-SNAI1 were injected weekly in the tail vein of the mice, respectively[29]. Mice in the PVR and Control groups were injected with equal doses of saline in the tail vein. The fundus of the mouse eye was examined weekly with a slit lamp and scored for PVR[30]. After 21d, all mice were executed by the guillotine method, and the eyeballs of mice were removed to collect and retinal tissue samples for backup.

Hematoxylin and Eosin Staining and MASSON Staining The retinal tissues were completely immersed in 4% paraformaldehyde, and then paraffin-embedded and serially sectioned 24h later. Sections were baked dry and placed in xylene (X821391, Macklin) to deparaffinize, then sequentially placed in graded ethanol solutions for rehydration. Staining with hematoxylin staining solution (H828282, Macklin) for 10min, and treated with differentiation solution (C0161s, Beyotime, Shanghai, China) for 30s. After washing, the sections were dyed with 1% eosin for 1min, then dehydration using gradient ethanol, transparent with xylene, and observed with a microscope.

Additionally, Masson's Trichrome Staining Kit (C0189S, Beyotime) was used to detect fibrosis in paraffin sections of mouse retinal tissue and to determine the number of cell nuclei in the outer nuclear layer (ONL) and inner nuclear layer (INL)[28].

Enzyme-Linked Immunosorbent Assay Human tumor necrosis factor-alpha (TNF-α, CB11762-Hu), interleukin (IL)-6 (CB10373-Hu), and IL-8 (CB10376-Hu) enzyme-linked immunosorbent assay (ELISA) kits; and mouse macrophage inflammatory protein (MIP)-1α (CB10426-Mu), MIP-1β (CB10430-Mu), IL-10 (CB10161-Mu), and IL-6 (CB10187-Mu) ELISA kits were purchased from Coibo Biotechnology (Shanghai, China). The ARPE-19 cell supernatant or homogenized tissue supernatant and the corresponding antibody were added into the ELISA well plate and incubated for 90min at 37°C[31]. HRP-labeled Streptavidin was added in the plate and incubated at 37°C away from light for 20min. After washed with washing solution, color agent A and B were added and incubated at 37°C for 15min. The termination agent was introduced and mixed, and the OD_{450} value was recorded.

Quantitative Reverse Transcription Polymerase Chain Reaction Mouse retinal tissues were lysed utilizing Trizol reagent (15596018CN, Invitrogen), reverse transcriptase (HY-KE8004, MedChemExpress) was applied for reverse transcription reaction to synthesize complementary DNA (cDNA). The cDNA was used as a template for PCR amplification using TB Green FAST qPCR (CN830S, TAKARA, Tokyo, Japan) on the PRISM 7300 RT-PCR system (ABI, Carlsbad, CA, USA). The target genes levels were quantified following the $2^{-\Delta\Delta Ct}$ method, with GAPDH served as a reference.

The primer sequences are detailed below: VRK1: F: 5'-TGGAAAAAGTTACAGGTTTATGATAATG-3'; R: 5'-GTAGTTTCACAGACTCCATGTACTTAGC-3'. GAPDH: F: 5'-CTTTGGCATTGTGGAAGGGC-3'; R: 5'-CAGGGATGATGTTCTGGGCA-3'.

Western Blot Mouse retinal tissues and ARPE-19 cells were thoroughly lysed using RIPA lysis buffer (20-188, Sigma-Aldrich). The protein concentration was examined using BCA Protein Quantification kit (B917925, Macklin). Next, proteins were separated by SDS-PAGE electrophoresis and transferred to a PVDF membrane (88518, Invitrogen), then blocked with 5% BSA for 2h. Subsequently, incubated with primary antibodies zonula occludens-1 (ZO-1, 61-7300, 1:2000,

Invitrogen), VRK1 (ab211358, 1:500, Abcam), E-cadherin (ab314063, 1:1000, Abcam), Collagen I (PA1-26204, 1:2000, Invitrogen), SNAI1 (MA5-14801, 1:1000, Invitrogen), matrix metalloproteinase (MMP) 2 (PA5-85197, 1:3000, Invitrogen), MMP9 (ab76003, 1:5000, Abcam) overnight at 4°C. The membrane was then incubated with the secondary antibody (ab205718, 1:10 000, Abcam) for 2h. Developing solution (HY-K2005, MedChemExpress) was dropped evenly on the membrane, and scanned with an iBright CL1500 gel imaging system (Invitrogen). GAPDH (MA5-35235, 1:50 000, Invitrogen) was used as an internal reference. Following image processing with Image J software, and relative expression levels were calculated.

Statistical Analysis Each experiment was repeated at least 3 times, and the experimental data were expressed as mean±standard deviation. Statistical analyses were performed using SPSS 26.0 software (IBM SPSS Statistics 26), and statistical graphs were drawn using GraphPad Prism 9 software. A one-way ANOVA was used to test the overall difference between the group means. Student's *t* test was employed to compare two groups, and Tukey's test to pairwise comparison between multiple groups. $P<0.05$ indicates statistical significance.

RESULTS

VRK1 Regulates TGF-β2-caused Proliferation and Migration of ARPE-19 Cells TGF-β2-treated cells showed typical EMT features, and the cell morphology was gradually transformed from regular polygonal epithelioid-like structure to shuttle- or spindle-shaped mesenchymal-like morphology (Figure 1A). Western blot indicated that TGF-β2 treatment caused a notable up-regulation of VRK1 protein (Figure 1B, 1C). Transfection of si-VRK1 decreased VRK1 level, whereas transfection of OE-VRK1 raised VRK1 level (Figure 1D, 1E). TGF-β2 treatment significantly raised the cellviability (Figure 1F) and EdU-positive rate (Figure 1G, 1H) of ARPE-19 cells, which was further enhanced by transfection of OE-VRK1; transfection of si-VRK1 declined cell viability and proliferation. Transwell (Figure 1I, 1J) and Scratch healing assay (Figure 1K, 1L) revealed that the migration ability of ARPE-19 cells was markedly increased after TGF-β2 treatment, and overexpression of VRK1 further enhanced the migration ability, whereas silencing VRK1 reversed these effects. These results indicate that interfering with VRK1 expression regulates TGF-β2-induced changes in cellular function, suggesting that VRK1 might be crucial in TGF-β2-mediated regulation of ARPE-19 cell phenotype and function.

VRK1 Modulates TGF-β2-caused Inflammation and EMT in ARPE-19 Cells ELISA results revealed that TGF-β2 treatment elevated IL-8, TNF-α, and IL-6 levels, overexpression of VRK1 further enhanced the release of inflammatory factors, while silencing VRK1 reversed these effects (Figure 2A-2C). TGF-β2 treatment notably increased the surface area and α-SMA fluorescence intensity of ARPE-19 cells. Overexpression of VRK1 further exacerbated the effect of TGF-β2, whereas silencing VRK1 effectively inhibited the above phenotypic changes (Figure 2D-2G). Additionally, after TGF-β2 intervention, SNAI1, α-SMA, and Collagen I, MMP2, and MMP9 were up-regulated, while ZO-1 and E-cadherin were decreased. Overexpression of VRK1 amplified the impact of TGF-β2; silencing VRK1 significantly reversed these proteins levels (Figure 2H, 2I). These results confirm that VRK1 is not only involved in TGF-β2-induced inflammatory responses, but also promotes EMT processes.

VRK1 Regulates SNAI1 Expression Transcription factor SNAI1 plays a key role in the EMT process[32]. TGF-β2 treatment markedly enhanced the SNAI1 fluorescence intensity, overexpression of VRK1 further elevated SNAI1 fluorescence intensity, whereas silencing VRK1 reversed this effect (Figure 3A, 3B). Additionally, Co-IP results showed that endogenous SNAI1 protein was efficiently captured when precipitated using VRK1 antibody; conversely, the presence of VRK1 protein was also detected when immunoprecipitated with SNAI1 antibody (Figure 3C). This result indicates that there is a direct interaction between VRK1 and SNAI1 in ARPE-19 cells.

Silencing VRK1 Hinders TGF-β2-caused Inflammation and EMT by Regulating SNAI1 Expression in ARPE-19 Cells After transfection of OE-SNAI1 in ARPE-19 cells, SNAI1 level was significantly elevated (Figure 4A, 4B). Transfection of si-VRK1 reduced the effect of TGF-β2 treatment, resulting in a lower proportion of EdU-positive cells; whereas transfection of OE-SNAI1 effectively reversed this effect (Figure 4C, 4D). Silencing VRK1 also significantly reduced cell migratory ability after TGF-β2 treatment, which was notably restored after transfection with OE-SNAI1 (Figure 4E-4H). We found that silencing VRK1 declined IL-6, TNF-α, and IL-8 levels, whereas transfection of OE-SNAI1 significantly raised inflammatory factor levels (Figure 4I-4K). Additionally, silencing VRK1 markedly reduced α-SMA and Collagen I levels; whiles overexpression of SNAI1 restored α-SMA and Collagen I levels (Figure 4L-4N). SNAI1 and α-SMA, Collagen I, MMP2 and MMP9 levels were markedly increased after transfection with OE-SNAI1, while the ZO-1 and E-cadherin levels were decreased (Figure 4O, 4P). The above findings confirmed that SNAI1 could alleviate the impacts of VRK1 silencing, further elucidating the central regulatory role of the VRK1/SNAI1 axis in TGF-β2-caused phenotypic transition of ARPE-19 cells.

Silencing VRK1 Inhibits Inflammation, EMT, and Retinal Detachment in PVR Mice Next, we constructed a mouse

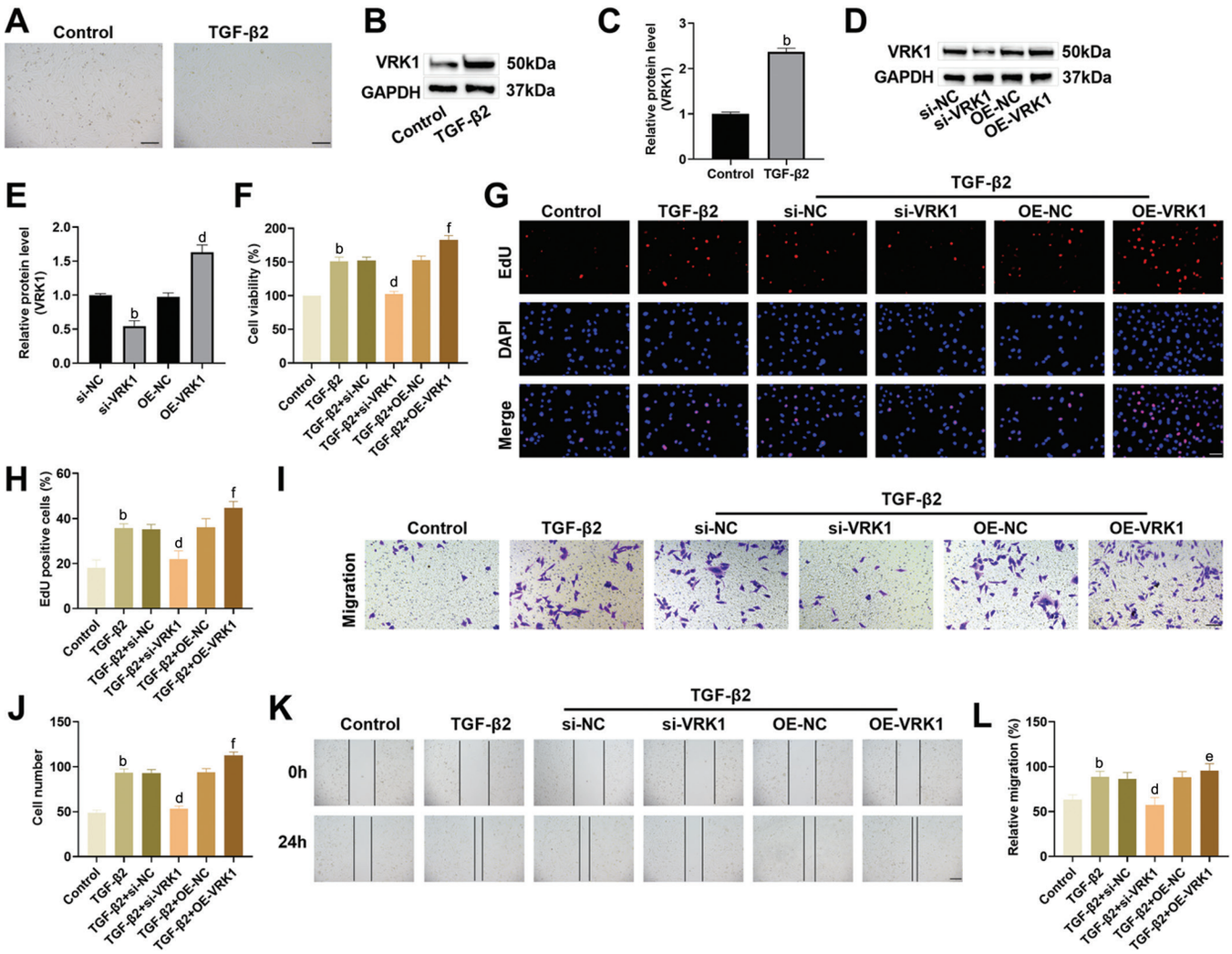

Figure 1 VRK1 regulates TGF-β2-caused proliferation and migration of ARPE-19 cells A: Observation of ARPE-19 cells under the light microscope (10×, 200 μm); B, C: Western blot measured VRK1 protein level; D, E: Western blot measured VRK1 protein level after transfection of si-VRK1/OE-VRK1; F: CCK-8 assay assessed ARPE-19 cell viability; G, H: EdU staining determined EdU-positive ARPE-19 cells after transfection of si-VRK1/OE-VRK1 (40×, 50 μm); I-L: Transwell assay (I, J) (20×, 100 μm) and Scratch-wound assay (K, L) (10×, 200 μm) measured ARPE-19 cell migration. n=3, ^{b}P<0.01 *vs* control; ^{d}P<0.01 *vs* TGF-β2+si-NC; ^{e}P<0.05, ^{f}P<0.01 *vs* TGF-β2+OE-NC. Student's *t*-test (C) or one-way ANOVA (E, F, H, J, L) was utilized. VRK1: Vaccinia-related kinase 1; TGF-β2: Transforming growth factor-β2; si-VRK1: VRK1 small interfering RNA; OE-VRK1: VRK1 overexpression; EdU: 5-Ethynyl-2'-deoxyuridine; ARPE-19: Human retinal pigment epithelial cell line.

model of PVR by injecting dispase. The retinal hierarchical structure of the PVR model mice was disorganized, with the thickness of the ONL and INL significantly reduced (Figure 5A-5C). VRK1 level was notably elevated in PVR mice, implying that VRK1 might be involved in the pathologic process of PVR (Figure 5D, 5E). Additionally, quantitative reverse transcription polymerase chain reaction (qRT-PCR) results demonstrated that si-VRK1 injection effectively reduced VRK1 mRNA levels (Figure 5F). PVR pathology scores showed that injection of si-VRK1 significantly attenuated pathological damage to retinal tissue (Figure 5G). MIP-1α, IL-6, and MIP-1β levels were notably elevated in PVR mice; injection of si-VRK1 notably decreased pro-inflammatory factor levels and increased IL-10 levels (Figure 5H-5K). Injection of si-VRK1 increased the density of ONL and INL cell nuclei in the retinas of PVR mice and improved the structural integrity of the retina and reduced the degree of pathologic damage (Figure 5L-5P). Additionally, ZO-1 and E-cadherin levels were notably down-regulated in PVR mice, whereas SNAI1, α-SMA, Collagen I, MMP2 and MMP9 was up-regulated, whereas injection of si-VRK1 reversed the above proteins expression (Figure 5Q, 5R). This confirms silencing of VRK1 ameliorates retinal pathologic damage by regulating inflammatory factors and EMT-related proteins in PVR mice.

VRK1 Mediates SNAI1 Regulation of Pathological Changes in PVR Mice SNAI1 level was markedly elevated in PVR mice, injection of si-VRK1 effectively reduced SNAI1 level, co-injection of OE-SNAI1 significantly attenuated

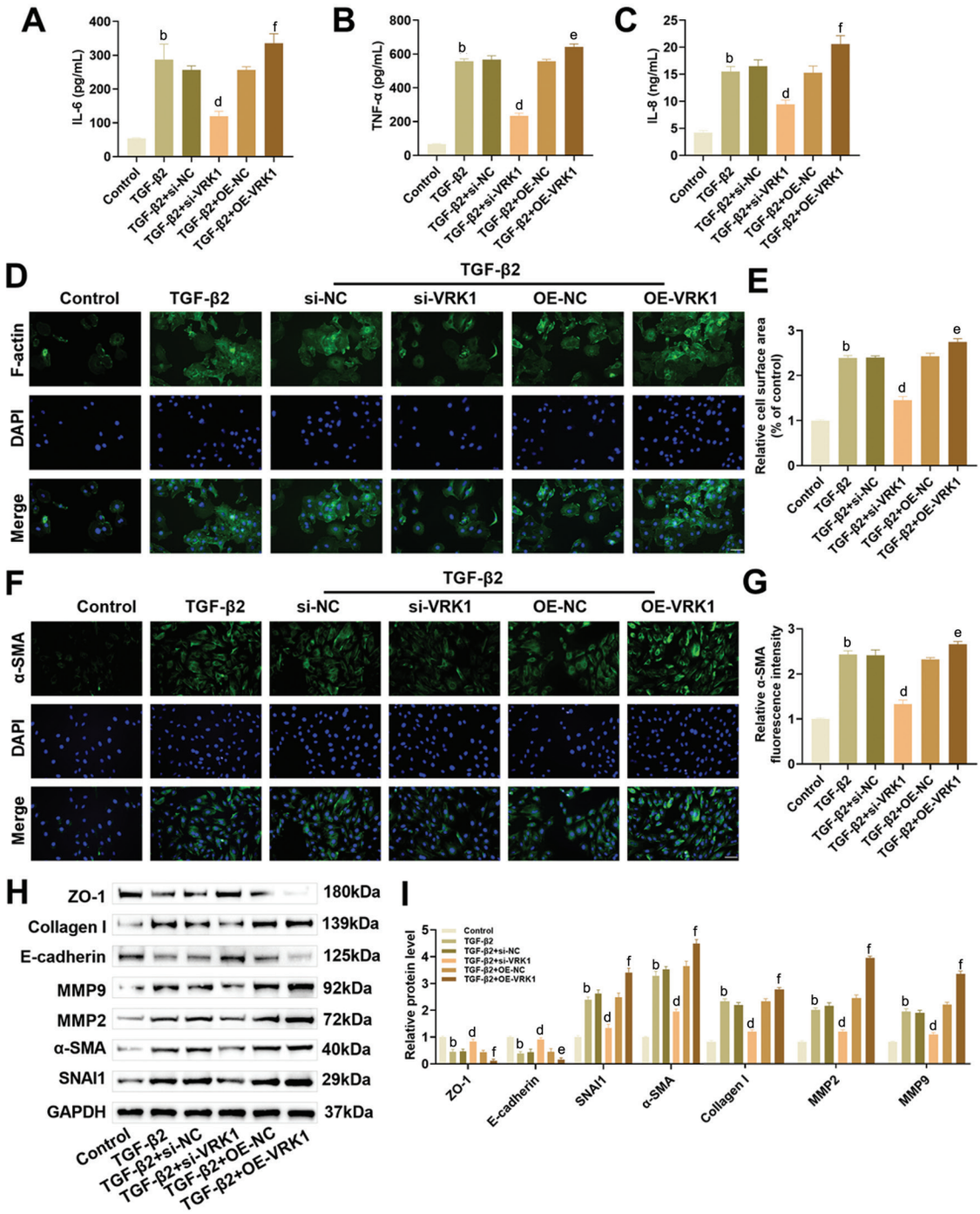

Figure 2 VRK1 regulates TGF-β2-caused inflammation and EMT in ARPE-19 cells A-C: IL-8, TNF-α, and IL-6 levels were measured by ELISA kits; D-G: Immunofluorescence measured surface area and α-SMA fluorescence intensity of ARPE-19 cells (40×, 50 μm); H, I: Western blot measured ZO-1, E-cadherin, SNAI1, α-SMA, Collagen I, MMP2, and MMP9 protein levels. n=3, ^{b}P<0.01 *vs* control; ^{d}P<0.01 *vs* TGF-β2+si-NC; ^{e}P<0.05, ^{f}P<0.01 *vs* TGF-β2+OE-NC. One-way ANOVA (A, B, C, E, G) or Tukey's test (I) was utilized. VRK1: Vaccinia-related kinase 1; TGF-β2: Transforming growth factor-β2; si-VRK1: VRK1 small interfering RNA; OE-VRK1: VRK1 overexpression; TNF-α: Tumor necrosis factor-alpha; IL: Interleukin; α-SMA: Alpha smooth muscle actin; SNAI1: Snail family transcriptional repressor 1; MMP: Matrix metalloproteinase; ZO-1: Zonula occludens-1; EMT: Epithelial-mesenchymal transition; ARPE-19: Human retinal pigment epithelial cell line.

the down-regulation effect of SNAI1 mediated by si-VRK1 (Figure 6A, 6B). Pathological staining showed that co-injection of OE-SNAI1 increased degree of retinal tissue damage, and the thickness of the ONL and INL was markedly reduced (Figure 6C-6G). After co-injection of OE-SNAI1, the pro-inflammatory factor levels were rebounded and IL-10 level was decreased (Figure 6H-6K). Additionally, overexpression of SNAI1 decreased ZO-1 and E-cadherin levels, and rebounded α-SMA, Collagen I, MMP2 and MMP9 expression (Figure 6L, 6M). These results indicate that overexpression of SNAI1 reverses the protective impact of silencing VRK1 on the retina of PVR mice.

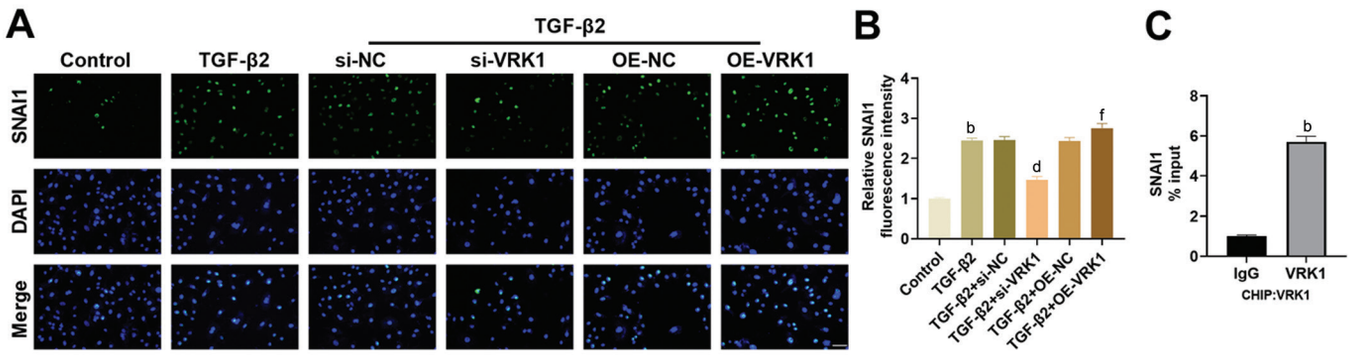

Figure 3 VRK1 regulates SNAI1 expression A, B: Immunofluorescence measured the fluorescence intensity of SNAI1 (40×, 50 μm); C: Co-IP assay measured a direct interaction between VRK1 and SNAI1. n=3, ^{b}P<0.01 *vs* control; ^{d}P<0.01 *vs* TGF-β2+si-NC; ^{f}P<0.01 *vs* TGF-β2+OE-NC. One-way ANOVA (B) or Student's t-test (C) was utilized. VRK1: Vaccinia-related kinase 1; TGF-β2: Transforming growth factor-β2; si-VRK1: VRK1 small interfering RNA; OE-VRK1: VRK1 overexpression; SNAI1: Snail family transcriptional repressor 1; Co-IP: Co-immunoprecipitation; ARPE-19: Human retinal pigment epithelial cell line.

DISCUSSION

RPE cells are among the primary contributors to the formation of PVR[33-34]. TGF-β triggers the transformation of RPE cells from epithelial cells to mesenchymal fibroblasts, resulting in a rise in the synthesis of extracellular matrix[8,35]. Research indicates that higher levels of TGF-β2 protein in the vitreous correlate positively with the severity of intraocular fibrosis in patients diagnosed with PVR[36-38]. In this study, we established a TGF-β2-induced EMT model in ARPE-19 cells and constructed a PVR mouse model by injecting dispase[21,27,39]. We observed that TGF-β2 treated ARPE-19 cells were transformed to mesenchymal fibroblasts, the proliferation and migration abilities were increased and mesenchymal-type proteins were up-regulated. Additionally, injection of dispase resulted in thickening of the preoptic membrane of the mouse retina and significant structural damage, confirming the successful construction of the PVR mouse model. Notably, VRK1 was upregulated in ARPE-19 cell model and PVR mouse model, suggesting that it may be involved in PVR progression.

EMT is a key pathophysiological change in embryonic development, tumor metastasis and various fibrotic diseases[40-42]. In PVR, EMT process of RPE cells is considered a central pathological event driving fibrous scar formation[43]. When the retina is subjected to pathological stimuli, the activated RPE cells separate from Bruch's membrane and migrate to the retinal neuroepithelial defect, where they undergo proliferation and transform into myofibroblasts, forming a fibro-proliferative membrane[31,44]. Zhu *et al*[45] found that VRK1 may be associated with the EMT process in a silicosis rat model. In our study, transfected OE-VRK1 further promoted TGF-β2-caused EMT phenotypic transformation of ARPE-19 cells, whereas transfected si-VRK1 reversed these manifestations. In PVR mice, injection of si-VRK1 effectively alleviated dispase-induced retinal histopathological damage and down-regulated mesenchymal marker levels, further confirming that down-regulating VRK1 could inhibit EMT during PVR progression.

Besides EMT, inflammation also markedly contributes to PVR progression[31,46]. Ni *et al*[47] showed that patients suffering from PVR exhibited notably increased concentrations of inflammatory markers. Luo *et al*[31] found that chemokines MIP-1α and MIP-1β levels were elevated in retinal tissues of PVR mice. The same trend was shown in our results, with increased levels of MIP-1α, IL-6, and MIP-1β in retinal tissues of PVR mice, which confirms that PVR progression accompanies the inflammatory response. Overexpression of VRK1 further promoted TGF-β2-caused inflammation in ARPE-19 cells, whereas silencing VRK1 reduced proinflammatory factor levels.

SNAI1 is regulated by multiple post-translational modifications and is important in a variety of fibrosis-related diseases[48-49]. In thymic epithelial tumors, overexpression of SNAI1 promoted cancer cell migration and EMT and enhanced stem cell-like properties of cancer cells[50]. Furthermore, overexpression of SNAI1 activated the NLRP3 inflammasome and promoted colitis, whereas inhibition of SNAI1 expression suppressed the inflammatory response[51]. Notably, VRK1 can increase SNAI1 expression in hepatocellular carcinoma cells by phosphorylating chromodomain helicase DNA binding protein 1 like (CHD1L), which in turn drives the EMT process[20]. We found that VRK1 expression in ARPE-19 cells was positively correlated with SNAI1 activity, and Co-IP assays also validated a direct interaction between VRK1 and SNAI1. Additionally, overexpression SNAI1 impaired the inhibitory impact of silencing VRK1 on PVR progression. Based on previous research reports[20], we hypothesize that VRK1 may inhibit the ubiquitin-mediated degradation of SNAI1 by directly binding to it and phosphorylating its specific sites.

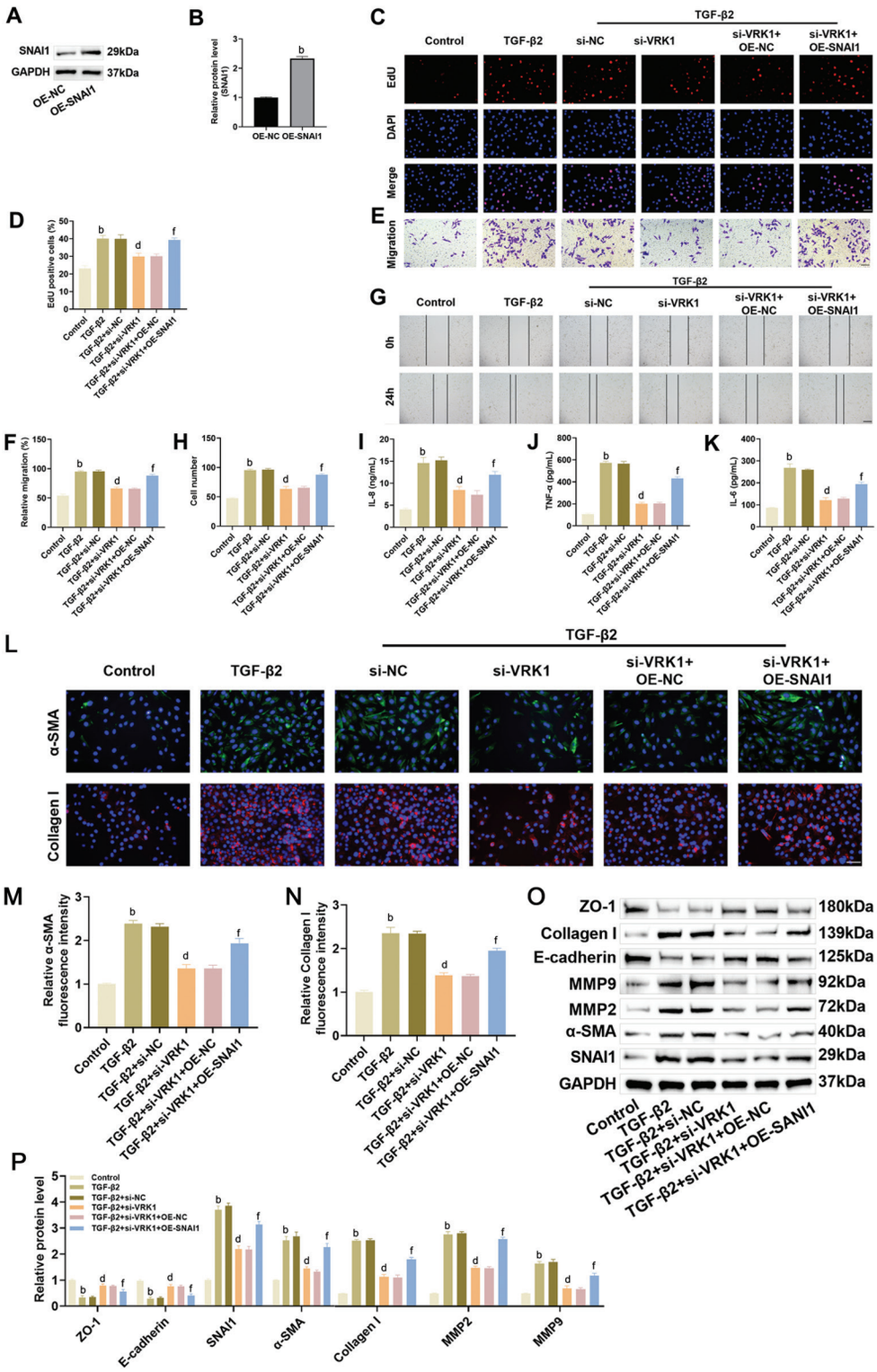

Figure 4 Silencing VRK1 hinders TGF-β2-caused inflammation and EMT by regulating SNAI1 expression in ARPE-19 cells A, B: SNAI1 protein level was examined through Western blot; C, D: EdU staining detected EdU-positive ARPE-19 cells after transfection of OE-SNAI1/si-VRK1 (40×, 50 μm); E-H: Cell migration was measured by Transwell assay (E, F) (20×, 100 μm) and Scratch-wound assay (G, H) (10×, 200 μm); I-K: ELISA kit measured IL-8, IL-6 and TNF-α levels; L-N: Immunofluorescence detected Collagen I and α-SMA levels in ARPE-19 cells (40×, 50 μm); O, P: Western blot measured ZO-1, E-cadherin, SNAI1, α-SMA, Collagen I, MMP2, and MMP9 levels in ARPE-19 cells. n=3, ^{b}P<0.01 *vs* control; ^{d}P<0.01 *vs* TGF-β2+si-NC; ^{f}P<0.01 *vs* TGF-β2+si-VRK1+OE-NC. Student's t-test (B), one-way ANOVA (D, F, H, I, J, K, M, N), or Tukey's test (P) were used. VRK1: Vaccinia-related kinase 1; TGF-β2: Transforming growth factor-β2; si-VRK1: VRK1 small interfering RNA; OE-VRK1: VRK1 overexpression; SNAI1: Snail family transcriptional repressor 1; OE-SNAI1: SNAI1 overexpression; EdU: 5-Ethynyl-2'-deoxyuridine; TNF-α: Tumor necrosis factor-alpha; IL: Interleukin; α-SMA: Alpha smooth muscle actin; SNAI1: Snail family transcriptional repressor 1; MMP: Matrix metalloproteinase; ZO-1: Zonula occludens-1; EMT: Epithelial-mesenchymal transition; ARPE-19: Human retinal pigment epithelial cell line.

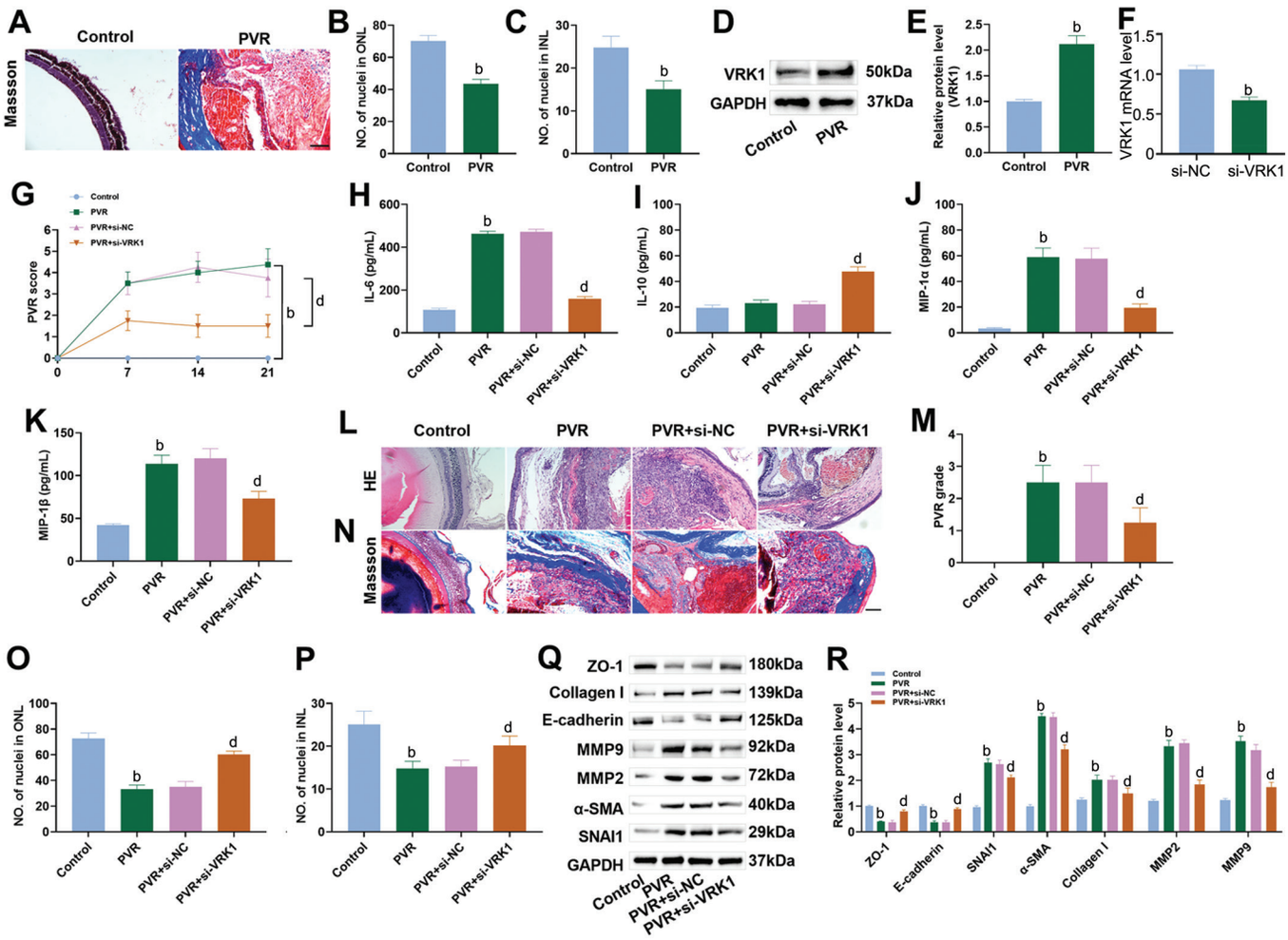

Figure 5 Silencing VRK1 inhibits inflammation, EMT, and retinal detachment in PVR mice A-C: Masson staining showed disrupted retinal structures in PVR mice, with reduced numbers of nuclei in the ONL and INL (20×, 100 μm); D-E: Western blot measured VRK1 levels in retinal tissue of PVR mice; F: qRT-PCR detection of VRK1 mRNA levels; G: PVR scores showed that injection of si-VRK1 improved pathological manifestations in retinal tissue of PVR mice; H-K: ELISA kits measured MIP-1α, IL-6, IL-10, and MIP-1β levels in the supernatants of retinal tissues from PVR mice; L-P: Retinal structural damage in PVR mice and the number of nuclei in the ONL and INL were observed by HE staining (L-M) and Masson staining (N-P) (20×, 100 μm); Q-R: Western blot measured ZO-1, E-cadherin, SNAI1, α-SMA, Collagen I, MMP2, and MMP9 levels. n=8, ^{b}P<0.01 *vs* control; ^{d}P<0.01 *vs* PVR+si-NC. Student's t-test (B, C, E, F), one-way ANOVA (G, H, I, J, K, M, O, P), or Tukey's test (R) were used. VRK1: Vaccinia-related kinase 1; EMT: Epithelial-mesenchymal transition; PVR: Proliferative vitreoretinopathy; si-VRK1: VRK1 small interfering RNA; HE: Hematoxylin and eosin; MIP: Macrophage inflammatory protein; SNAI1: Snail family transcriptional repressor 1; IL: Interleukin; ONL: Outer nuclear layer; INL: Inner nuclear layer; ZO-1: Zonula occludens-1; α-SMA: Alpha smooth muscle actin; MMP: Matrix metalloproteinase; SNAI1: Snail family transcriptional repressor 1; ARPE-19: Human retinal pigment epithelial cell line.

In vitro, TGF-β2-caused upregulation of VRK1 could drive the EMT process and inflammatory response in RPE cells by activating SNAI1; *in vivo*, silencing VRK1 ameliorated retinal histopathological damage and inflammatory response in PVR mice by down-regulating SNAI1. The above findings reveal the regulatory role of the VRK1/SNAI1 axis in the pathological process of PVR. However, the pathogenesis of PVR is very complex, and the interaction of the VRK1/SNAI1 axis with other PVR-related signaling pathways will be further explored in the future.

ACKNOWLEDGEMENTS

Authors' Contributions Ying Y, Liao X: Conducted and designed the research, carried out experiments, and analyzed findings. Edited and refined the manuscript with a focus on critical intellectual contributions. Ying Y, Liao X: Participated in collecting, assessing, and interpreting the data. Made significant contributions to data interpretation and manuscript preparation. Liao X: Provided substantial intellectual input during the drafting and revision of the manuscript. The final version of the manuscript has been reviewed and approved by all authors.

Availability of Data and Materials: The data supporting the findings of this study can be obtained from the corresponding author, Liao X, upon request.

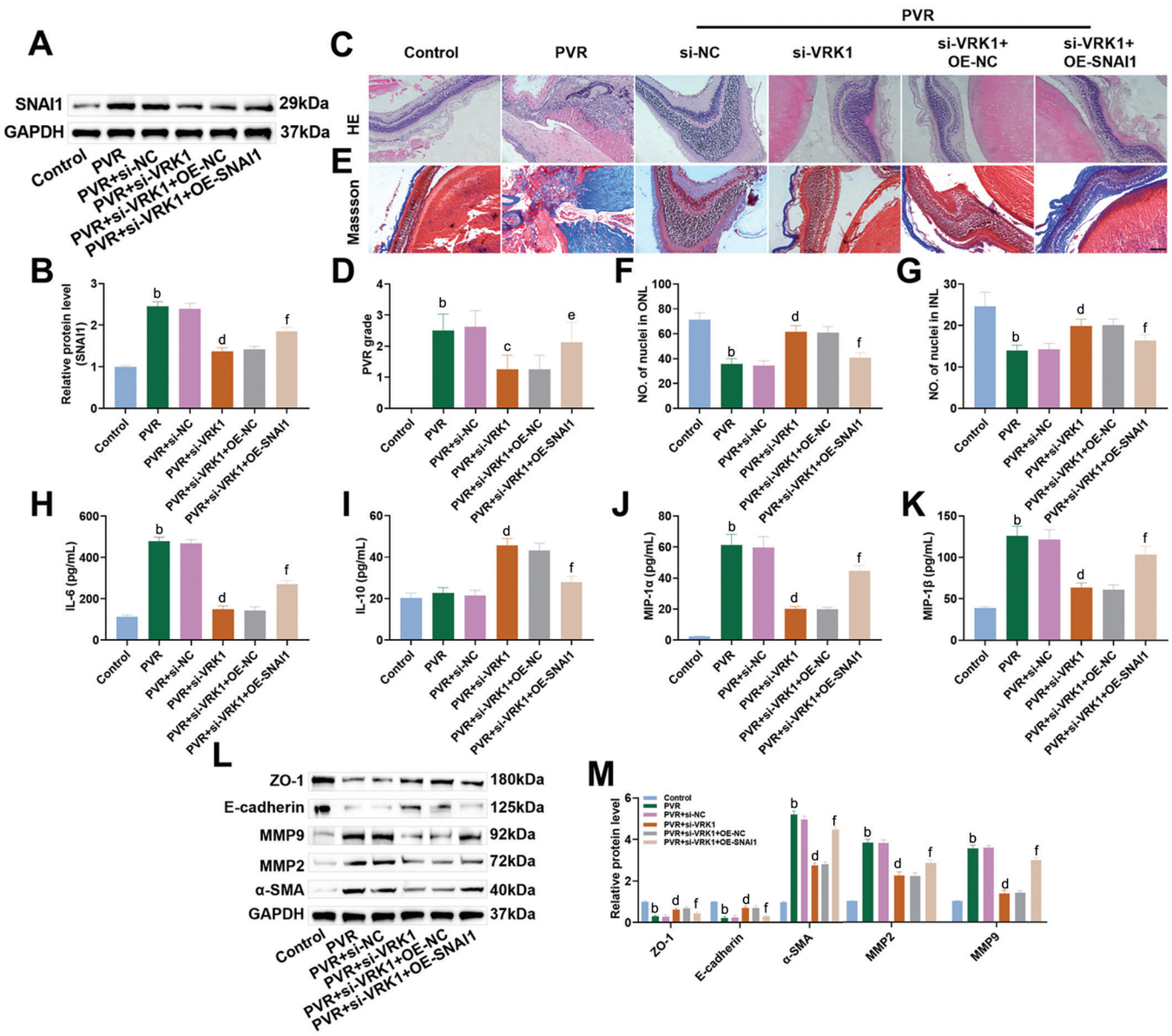

Figure 6 VRK1 mediates SNAI1 regulation of pathological changes in PVR mice A, B: Western blot measured SNAI1 expression in PVR mice; C-G: Retinal structural damage and the number of nuclei were observed by HE staining (C-D) and Masson staining (E-G) (40×, 50 μm); H-K: ELISA kits measured MIP-1α, IL-6, IL-10, and MIP-1β levels; L, M: Western blot measured ZO-1, E-cadherin, α-SMA, MMP2, and MMP9 levels. n=8, ^{b}P<0.01 *vs* control; ^{c}P<0.05, ^{d}P<0.01 *vs* PVR+si-NC; ^{e}P<0.05, ^{f}P<0.01 *vs* PVR+si-VRK1+OE-NC. One-way ANOVA (B, D, F, G, H, I, J, K) or Tukey's test (M) was employed. VRK1: Vaccinia-related kinase 1; EMT: Epithelial-mesenchymal transition; PVR: Proliferative vitreoretinopathy; si-VRK1: VRK1 small interfering RNA; HE: Hematoxylin and eosin; MIP: Macrophage inflammatory protein; SNAI1: Snail family transcriptional repressor 1; IL: Interleukin; ONL: Outer nuclear layer; INL: Inner nuclear layer; ZO-1: Zonula occludens-1; α-SMA: Alpha smooth muscle actin; MMP: Matrix metalloproteinase; OE-SNAI1: SNAI1 overexpression; ARPE-19: Human retinal pigment epithelial cell line.

Conflicts of Interest: Ying Y, None; **Liao X,** None.

REFERENCES

1 Ferro Desideri L, Artemiev D, Zandi S, *et al*. Proliferative vitreoretinopathy: an update on the current and emerging treatment options. *Graefes Arch Clin Exp Ophthalmol* 2024;262(3):679-687.

2 Martinez Pacheco VA, Rojas Juarez S, Velasco Sepulveda BH, *et al*. Proliferative vitreoretinopathy and its relationship with inflammatory serum biomarkers. *Int J Ophthalmol* 2024;17(9):1659-1664.

3 Carpineto P, Licata AM, Ciancaglini M. Proliferative vitreoretinopathy: a reappraisal. *J Clin Med* 2023;12(16):5287.

4 Wu F, Eliott D. Molecular targets for proliferative vitreoretinopathy. *Semin Ophthalmol* 2021;36(4):218-223.

5 Assi A, Charteris D. Proliferative vitreoretinopathy: a revised concept of retinal injury and response. *Br J Ophthalmol* 2024;108(12):1621-1626.

6 Sabatino F, Banerjee P, K Muqit MM. Clinical therapeutics for proliferative vitreoretinopathy in retinal detachment. *Surv Ophthalmol* 2024;69(4):508-520.

7 Dhawale KK, Tidake P. Advancements in therapeutic approaches for proliferative vitreoretinopathy: a comprehensive review. *Cureus* 2024;16(7):e65893.

8 Sreenivas Bk A, Simakurthy S, Shanmugam PM, *et al*. Commonalities between fibrotic and inflammatory mechanisms in proliferative vitreoretinopathy and proliferative diabetic retinopathy. *Exp Eye Res* 2025;258:110482.

9 Lin JB, Wu F, Kim LA. Proliferative vitreoretinopathy: pathophysiology and therapeutic approaches. *Int Ophthalmol Clin* 2024;64(2):125-135.

10 Ma X, Xie Y, Gong Y, *et al*. Silibinin prevents TGFβ-induced EMT of RPE in proliferative vitreoretinopathy by inhibiting Stat3 and Smad3 phosphorylation. *Invest Ophthalmol Vis Sci* 2023;64(13):47.

11 Ma X, Han S, Liu Y, *et al*. DAPL1 prevents epithelial–mesenchymal transition in the retinal pigment epithelium and experimental proliferative vitreoretinopathy. *Cell Death Dis* 2023;14:158.

12 Yue YK, Chen XL, Liu S, *et al*. Upregulation of ASPP2 expression alleviates the development of proliferative vitreoretinopathy in a rat model. *Int J Ophthalmol* 2021;14(12):1813-1819.

13 Harju N, Kauppinen A, Loukovaara S. Fibrotic changes in rhegmatogenous retinal detachment. *Int J Mol Sci* 2025;26(3):1025.

14 Zhou M, Geathers JS, Grillo SL, *et al*. Role of epithelial-mesenchymal transition in retinal pigment epithelium dysfunction. *Front Cell Dev Biol* 2020;8:501.

15 Li D, Yuan D, Shen H, *et al*. Gremlin-1: an endogenous BMP antagonist induces epithelial-mesenchymal transition and interferes with redifferentiation in fetal RPE cells with repeated wounds. *Mol Vis* 2019;25:625-635.

16 Gharegezloo Z, Rezvani Z, Sanie-Jahromi F, *et al*. The effect of *Coix lachrymal L*. seed extract on the expression of inflammation and fibrogenesis genes in human retinal pigment epithelial cells. *Biomed Pharmacother* 2024;181:117646.

17 Chang X, Tamauchi S, Yoshida K, *et al*. Downregulating vaccinia-related kinase 1 by luteolin suppresses ovarian cancer cell proliferation by activating the p53 signaling pathway. *Gynecol Oncol* 2023;173:31-40.

18 Carrión-Marchante R, Frezza V, Salgado-Figueroa A, *et al*. DNA aptamers against vaccinia-related kinase (VRK) 1 block proliferation in MCF7 breast cancer cells. *Pharmaceuticals* (*Basel*) 2021;14(5):473.

19 Sun X, Zhao W, Wang Q, *et al*. Inhibition of VRK1 suppresses proliferation and migration of vascular smooth muscle cells and intima hyperplasia after injury *via* mTORC1/β-catenin axis. *BMB Rep* 2022;55(5):244-249.

20 Li J, Song Z, Dong X, *et al*. VRK1 promotes epithelial-mesenchymal transition in hepatocellular carcinoma mediated by SNAI1 *via* phosphorylating CHD1L. *Cell Death Dis* 2025;16(1):302.

21 Yin Y, Liu S, Pu L, *et al*. Nintedanib prevents TGF-β2-induced epithelial-mesenchymal transition in retinal pigment epithelial cells. *Biomedecine Pharmacother* 2023;161:114543.

22 Cinar AK, Ozal SA, Serttas R, *et al*. Eupatilin attenuates TGF-β2-induced proliferation and epithelial-mesenchymal transition of retinal pigment epithelial cells. *Cutan Ocul Toxicol* 2021;40(2):103-114.

23 Shen Z, Zhao L, Yoo SA, *et al*. Emodin induces ferroptosis in colorectal cancer through NCOA4-mediated ferritinophagy and NF-κb pathway inactivation. *Apoptosis* 2024;29(9-10):1810-1823.

24 Xu R, Yang L, Song G. Plectin promotes the migration of hepatocellular carcinoma cells through inducing F-actin polymerization. *J Sichuan Univ Med Sci Ed* 2024;55(1):60-66.

25 Liu T, Xu P, Ke S, *et al*. Histone methyltransferase SETDB1 inhibits TGF-β-induced epithelial-mesenchymal transition in pulmonary fibrosis by regulating SNAI1 expression and the ferroptosis signaling pathway. *Arch Biochem Biophys* 2022;715:109087.

26 Park SM, Park SH, Ryu KJ, *et al*. Downregulation of CHIP promotes ovarian cancer metastasis by inducing Snail-mediated epithelial-mesenchymal transition. *Mol Oncol* 2019;13(5):1280-1295.

27 Young AP, Szczesniak AM, Hsu K, *et al*. Enantiomeric agonists of the type 2 cannabinoid receptor reduce retinal damage during proliferative vitreoretinopathy and inhibit hyperactive microglia *in vitro*. *ACS Pharmacol Transl Sci* 2024;7(5):1348-1363.

28 Yoo K, Son BK, Kim S, *et al*. Substance P prevents development of proliferative vitreoretinopathy in mice by modulating TNF-α. *Mol Vis* 2017;23:933-943.

29 Xiong J, Ling J, Yan J, *et al*. LILRB4 knockdown inhibits aortic dissection development by regulating pyroptosis and the JAK2/STAT3 signaling pathway. *Sci Rep* 2024;14(1):15564.

30 Chen SH, Lin YJ, Wang LC, *et al*. Doxycycline ameliorates the severity of experimental proliferative vitreoretinopathy in mice. *Int J Mol Sci* 2021;22(21):11670.

31 Luo M, Almeida D, Dallacasagrande V, *et al*. Annexin A2 promotes proliferative vitreoretinopathy in response to a macrophage inflammatory signal in mice. *Nat Commun* 2024;15(1):8757.

32 Zhang X, Luo Y, Cen Y, *et al*. MACC1 promotes pancreatic cancer metastasis by interacting with the EMT regulator SNAI1. *Cell Death Dis* 2022;13(11):923.

33 Idrees S, Sridhar J, Kuriyan AE. Proliferative vitreoretinopathy: a review. *Int Ophthalmol Clin* 2019;59(1):221-240.

34 Zong T, Mu T, Tan CY, *et al*. Tenascin-C induces transdifferentiation of retinal pigment epithelial cells in proliferative vitreoretinopathy. *Exp Eye Res* 2024;248:110097.

35 Hachana S, Larrivée B. TGF-β superfamily signaling in the eye: implications for ocular pathologies. *Cells* 2022;11(15):2336.

36 Wu L, Yang S, Li H, *et al*. TSPAN4-positive migrasome derived from retinal pigmented epithelium cells contributes to the development of proliferative vitreoretinopathy. *J Nanobiotechnology* 2022;20(1):519.

37 Zhao Z, Zhang Y, Zhang C, *et al*. TGF-β promotes pericyte-myofibroblast transition in subretinal fibrosis through the Smad2/3 and Akt/mTOR pathways. *Exp Mol Med* 2022;54(5):673-684.

38 Wang G, Zhao R, Guo Z, *et al*. Autophagy activation ameliorates the fibrosis of trabecular meshwork cells induced by TGFβ2 through the promotion of fibrotic proteins degradation. *Hum Cell* 2024;38(1):4.

39 Datlibagi A, Zein-El-Din A, Frohly M, *et al*. Experimental models to study epithelial-mesenchymal transition in proliferative vitreoretinopathy. *Int J Mol Sci* 2023;24(5):4509.

40 Youssef KK, Nieto MA. Epithelial-mesenchymal transition in tissue repair and degeneration. *Nat Rev Mol Cell Biol* 2024;25(9):720-739.

41 Wei Z, Babkirk K, Chen S, *et al*. Epithelial-to-mesenchymal transition transcription factors: New strategies for mesenchymal tissue regeneration. *Cytokine Growth Factor Rev* 2025;83:99-124.

42 Yousefnia S. Mechanistic role of circRNAs in malignant characterizations of cancer stem cells. *J Can Biomol Therap* 2025;2(3):19-28.

43 Jiang H, Chen Y, He Z, *et al*. Targeting non-muscle myosin II inhibits proliferative vitreoretinopathy through regulating epithelial-mesenchymal transition. *Biochem Biophys Res Commun* 2023;686:149149.

44 Gelat B, Rathaur P, Malaviya P, *et al*. The intervention of epithelial-mesenchymal transition in homeostasis of human retinal pigment epithelial cells: a review. *J Histotechnol* 2022;45(4):148-160.

45 Zhu Y, Yao J, Duan Y, *et al*. Protein expression profile in rat silicosis model reveals upregulation of PTPN2 and its inhibitory effect on epithelial-mesenchymal transition by dephosphorylation of STAT3. *Int J Mol Sci* 2020;21(4):1189.

46 Zhao YM, Sun RS, Duan F, *et al*. Intravitreal slow-release dexamethasone alleviates traumatic proliferative vitreoretinopathy by inhibiting persistent inflammation and Müller cell gliosis in rabbits. *Int J Ophthalmol* 2023;16(1):22-32.

47 Ni Y, Qin Y, Huang Z, *et al*. Distinct serum and vitreous inflammation-related factor profiles in patients with proliferative vitreoretinopathy. *Adv Ther* 2020;37(5):2550-2559.

48 Wang P, Kang Q, Wu W, *et al*. Hepatic Snai1 and Snai2 promote liver regeneration and suppress liver fibrosis in mice. *Cell Rep* 2024;43(3):113875.

49 Dong B, Wu Y. Epigenetic regulation and post-translational modifications of SNAI1 in cancer metastasis. *Int J Mol Sci* 2021;22(20):11062.

50 Haoran HR, Zhang L, Yang ZH, *et al*. SNAI1 promotes epithelial-mesenchymal transition and maintains cancer stem cell-like properties in thymic epithelial tumors through the PIK3R2/p-EphA2 Axis. *J Exp Clin Cancer Res* 2024;43(1):324.

51 Wang T, Liu W, Li C, *et al*. Mist1 promoted inflammation in colitis model *via* K^+-ATPase NLRP3 inflammasome by SNAI1. *Pathol Res Pract* 2021;224:153511.